Observation of a Phase Transition in the Sedimentation Velocity of Hard Spheres

S. E. Paulin and Bruce J. Ackerson
Department of Physics, Oklahoma State University, Stillwater, Oklahoma 74078
(Received 16 January 1990)

Reduced sedimentation velocities are reported for suspensions of nearly hard PMMA (polymethylmethacrylate) spheres as a function of volume fraction. The absolute sedimentation velocities are sufficiently slow compared to crystal-growth rates so that phase separation is achieved during the sedimentation process. As a result the analytic behavior of the measured sedimentation velocity changes as a function of volume fraction at the freezing and melting points. This transition serves as a definitive marker for comparison with theoretical predictions of sedimentation velocities for hard-sphere liquids and crystals.

PACS numbers: 64.60.Cn, 05.70.Fh, 64.70.Dv

The hard-sphere interaction of particles provides a simple but rich and important statistical-mechanical model of condensed matter. The melting-freezing transition has been demonstrated via molecular dynamics[1] and studied most recently via density-functional theory.[2] The liquid phase structure is modeled by the Wertheim-Thiele[3] solution to the Percus-Yevick equation, and the Carnahan-Starling equation[4] correlates the thermodynamic results of computer simulations. In hard-sphere perturbation theory, many of these results are used as the basis for calculating more accurate thermodynamic properties in a perturbation expansion about the hard-sphere state.[5-7] In general, these approximations are necessary because no particles interact via a true hard-sphere potential. However, recently the thermodynamics and statistical properties of ideal hard-sphere systems have been used to interpret the results of experiments on colloidal suspensions of sterically stabilized particles.[8-13] These particles interact via a short-ranged repulsive interaction with the stabilizing layer mitigating any van der Waals attractive forces. Compared to the charge stabilized interactions of colloidal particles or the typical interactions of atomic particles, these interactions may prove to be the best realization of the hard-sphere potential.

The nonequilibrium properties of suspended particles differ from those for purely atomic systems due to the presence of a solvent which transmits hydrodynamical forces. Much theoretical work has been directed toward understanding nonequilibrium properties of model hard-sphere suspensions,[14-20] again providing a basis for understanding more complex systems having other interparticle interactions. Experimental data for nonequilibrium processes in suspensions of hard spheres are limited but serve as an important check of theoretical results.

In this Letter we report values for the sedimentation velocity of "hard" spheres which equilibrate locally, forming liquidlike or polycrystalline ordering of particles before significant sedimentation is observed. As a result, measurements of the sedimentation velocity have been made for randomly stacked polycrystalline phases at large volume fraction and for liquidlike phases at low volume fractions. The melting-freezing phase transition is observed in the reduced sedimentation velocity as a function of the particle volume fraction and serves as a definitive marker for comparison with theoretical results. These experimental results differ in one aspect or another from others reported for "hard"-sphere suspensions[8-13,21,22] in that our results extend to large volume fractions, the particles are not charged, and we do observe the melting-freezing transition. The failure to observe a melting-freezing transition in other work may have resulted from not having hard-sphere interactions, a polydispersity of particle size, or a sedimentation rate greater than the nucleation and growth rate for crystallites. The last condition will result in an amorphous interparticle ordering during sedimentation despite the lower free energy of the equilibrium crystal phase. An order-disorder transition has been reported for the sedimentation of hard spheres,[9,22] but this is a sedimentation-induced crystallization where the increase in particle concentration on sedimentation triggers crystallization.[15]

The "hard" particles used in these studies are 0.99-μm-diam polymethylmethacrylate (PMMA) spheres having a relative standard deviation to mean radius less than 0.05, sterically stabilized with an approximately 10-nm-thick coating of poly-12-hydroxylstearic acid,[23,24] and suspended in a mixture of decaline and tetralin in a ratio chosen to closely match the index of refraction of the particles. The resulting suspensions are nearly transparent even up to volume fractions (ϕ) greater than 0.70, allowing for the visual observation of crystallite formation, the visual observation of sedimentation boundaries, and light-diffraction studies of particle microstructure. Samples ranging in volume fraction of particles from $\phi \sim 0.42$ to ~ 0.60 were made by the centrifugation of 4-cm^3 cuvettes filled with an index-matched stock sample of known sphere volume fraction and removal of supernatant to achieve the target volume fractions. For the sedimentation measurements the cuvettes are tumbled to

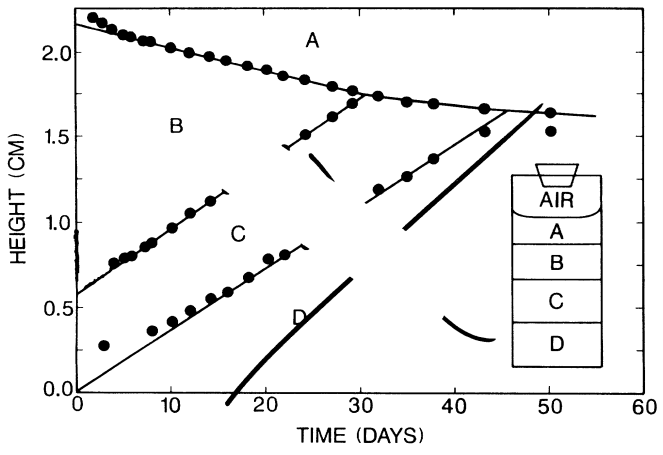

FIG. 1. A representative height vs time plot of a sample with its initial volume fraction ($\phi = 0.49$) within the coexistence region. *A*, clear supernatant; *B*, liquid; *C*, polycrystalline solid; and *D*, high-density polycrystalline sediment.

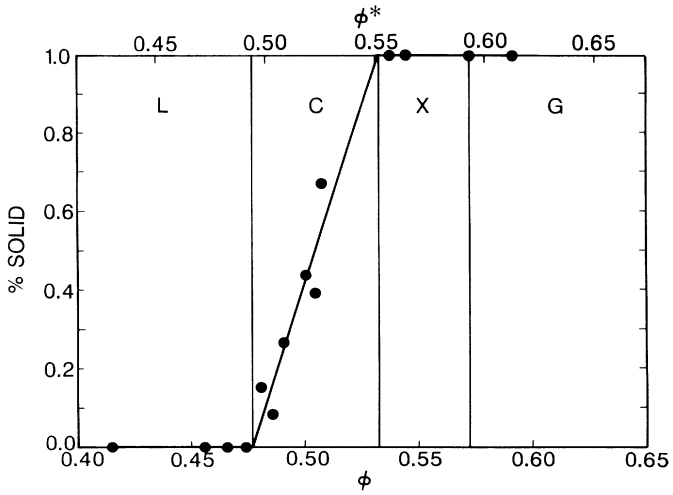

FIG. 2. Phase diagram obtained from suspensions. Scaled and measured volume fractions are shown on the upper and lower horizontal axis, respectively. *L* is liquid, *C* coexistence, *X* crystal, and *G* glass.

redisperse the particles and left to stand a period of two months at room temperature (22 ± 1 °C), except for careful periodic weighing to monitor any solvent vapor leakage. After a few days a typical sample will evidence the formation of several distinct layers as depicted in the lower right-hand corner of Fig. 1. The number of layers and the particle microstructure within a layer depends on the initial volume fraction. We observe four distinct types of height versus time diagrams as shown in Fig. 1, corresponding to the different equilibrium phases noted in Fig. 2. Here *L*, *C*, *X*, and *G* are liquid, coexisting liquid and crystal, fully crystalline, and glass phases. The height versus time diagram in Fig. 1 is typical for samples in the coexisting region, $0.477 < \phi < 0.533$ of Fig. 2, where the regions are defined to be (*A*) clear supernatant, (*B*) liquid, (*C*) polycrystalline solid, and (*D*) high-density polycrystalline sediment. The volume fraction of region *D* for samples in the coexistence region is found to be less than closest packing for hard spheres due to the random settling of individual crystallites which may not fit together in closest-packed formation and/or due to compressive distortion of the crystal microstructure which prevents closest packing. In Fig. 1, for samples in the liquid phase, $\phi < 0.477$, region *C* is not present and region *D* shows columnar crystal growth. For $0.533 < \phi < 0.573$ the samples are fully crystalline, region *B* being negligibly small and presumed to be caused by shear melting when weighing. For $\phi > 0.573$ there are no distinct boundaries and the sample is amorphous or glassy, failing to crystallize, except for a small region at the very top, during the time scale of our measurements. Sedimentation measurements are extended to $\phi = 0.099$ by successive dilutions of one of these samples ($\phi = 0.415$). In Fig. 1 the initial nonlinearity in the *A*/*B* boundary results from the curvature of the air-sample miniscus. On the other hand, the nonlinearity in the *B*/*C* boundary results from the initial nucleation and settling of crystallites throughout the entire sample.

The phase diagram in Fig. 2 is constructed by extrapolating the linear portion of the layer boundaries to zero time. In this limit only crystal (*C*) and/or liquid (*B*) regions exist, regions *A* and *D* having extrapolated to zero volume. Thus the crystal fraction may be determined unambiguously and should correspond to that in the absence of settling. Figure 2 presents the percent crystal versus volume fraction ϕ. The freezing and melting points are found to be $\phi_f = 0.477$ and $\phi_m = 0.533$, respectively, using a linear-regression fit to the coexistence region data. The results for hard-sphere phase behavior, determined by computer simulations,[1] give the freezing and melting volume fractions to be 0.494 and 0.545, respectively. The lack of agreement with our results indicates a possible increase in particle size due to adsorbtion of the solvent onto the stabilizing layer, which is not included in the dry-weight determination of ϕ, or to a deviation from true hard-sphere interactions.[8] Pusey and van Megen[8] have observed a larger discrepancy for smaller diameter particles having the same steric stabilizer but suspended in decalin and CS_2. To account for possible solvent adsorption and to compare with hard-sphere theory, they scale the measured volume fraction to coincide with the theoretical hard-sphere freezing point. Following this same procedure we scale our volume fractions using $\phi^* = (0.494/0.477)\phi$ as shown on the upper horizontal axis of Fig. 2. It is interesting to note that this corresponds to an effective radius increment for the particles of only ~ 6 nm.

Sedimentation velocities of the liquid and crystal are

calculated from the linear regions of the boundary lines shown in Fig. 1. For the liquid ($\phi^* < \phi_f^*$) and for the fully crystalline samples ($\phi_m^* < \phi^*$), the sedimentation velocity is given directly by the slope of the uppermost boundary A/B and A/C, respectively, in the height versus time diagram. For the coexistence region the liquid sedimentation velocity is determined as above and the crystal sedimentation velocity is determined from the B/C boundary using particle conservation, from which one may show the velocity of the settling crystal phase to be $(\phi_f^*/\phi_m^*)(v_{mc}+v_{ml})-v_{mc}$, where ϕ_m^* and ϕ_f^* are the melting and freezing volume fractions, respectively, and v_{mc} and v_{ml} the measured boundary velocities of the B/C and A/B boundaries, respectively. The crystal sedimentation velocity has also been estimated from the A/C boundary after region B has completely sedimented into C. While there is general agreement with the two estimates of the sedimentation velocity, the height versus time data for the A/C boundary is limited and evidenced a larger variation.

The measured sedimentation velocities are normalized to the sedimentation rate of an isolated sphere, $v_{\text{Stokes}} = 2ga^2(\rho_p-\rho_s)/9\eta$, where g is the acceleration due to gravity, ρ_p and ρ_s are the density of the sphere and solvent, respectively, η is the solvent viscosity (2.28×10^{-3} Pas at 22°C), and a is the sphere radius. The reduced sedimentation velocity is given by $K = v_{\text{meas}}/v_{\text{Stokes}}$ and is plotted in Fig. 3(a) as a function of ϕ^*. The data for $\phi^* < \phi_f^*$, in the liquid region, agree with previous experimental results for hard spheres.[13,21,25] In Fig. 3(b), for $\phi_f^* < \phi^* < \phi_m^*$ two reduced sedimentation velocities are shown at each ϕ^* value measured. The upper corresponds to the liquid phase and the lower to the crystalline phase. It is seen that the sedimentation rates of the liquid and crystalline phases are independent of ϕ^*. Because sedimentation velocities are a function of volume fraction and in the coexistence region the fluid and crystalline volume fractions are fixed at ϕ_f^* and ϕ_m^*, respectively, these ϕ^*-independent sedimentation velocities should be expected. This observation serves as a marker for the phase transition and could be used in other systems to confirm or establish a phase transition when other measurements are not easy or possible. Furthermore, the phase diagram is used to define the liquid ϕ_f^* and solid ϕ_m^* volume fractions uniquely. For $\phi^* > \phi_m^*$ the reduced sedimentation velocity corresponds to that for the polycrystalline solid phase. The $\phi^* = 0.593$ and 0.613 points correspond to glass samples which never crystalized during our period of observation.

A number of empirical formulas have been presented to correlate settling data for hard spheres.[19-21] Only relatively recently have more rigorous microscopic theories been developed.[16,18] However, the many-body nature of the hydrodynamic interaction ultimately necessitates using approximations to calculate the reduced sedimentation velocity. In Fig. 3(a), for $\phi^* < \phi_f^*$, the data are

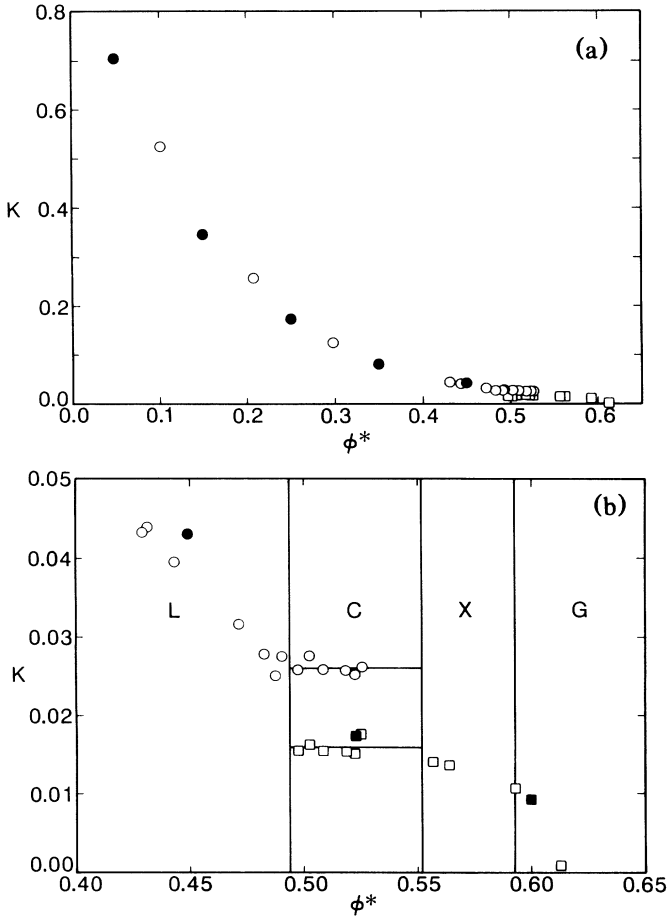

FIG. 3. (a) The reduced sedimentation velocity data of liquid (○) and crystal (□) are shown as a function of scaled volume fraction with the theory of Beenakker and Mazur (Ref. 18) (●). (b) Close-up of the transition region with the theory of Zick and Homsy (Ref. 26) (■), L being liquid, C coexistence, X crystal, and G glass regions.

compared with the theoretical results of Beenakker and Mazur.[18] In this theory N-body hydrodynamic interactions are included with spatial correlations taken only at a pairwise level in evaluating the result. Furthermore, a form for the sedimentation velocity is used which neglects memory function effects. Thus "zero g" equilibrium particle-distribution functions are assumed for evaluation of any ensemble averages. Despite these approximations the comparison with this theory and other data is quite good. For $\phi^* > \phi_f^*$ in the crystalline phase, our data may be compared with calculations of the hydrodynamic resistance of a rigid, oriented, single-crystal structure.[26,27] In Fig. 3(b) the results of Zick and Homsy[26] for an fcc crystal with the [100] direction parallel to the average flow are shown. The agreement with our data is again seen to be quite good despite our samples being randomly oriented, polycrystals having a close-

packed-random-stacked order. Furthermore, our particles are not constrained to fixed lattice positions. In this regard, we note that Saffman has shown in dilute suspensions that thermal motion and response to flow can have a significant effect.[28] Also, it should be noted that the data are measured and theory calculated in the same volume-fixed reference frame, and so no reference-frame corrections have been necessary to compare theory with experiment.

A limited number of scattering measurements have been made from the crystal (C) and dense sedimentary (D) structures. At the times when sedimentation velocities are measured, the crystal structures are uniform in density exhibiting little or no variation of density with height. The dense sediment does not appear isotropic, in general, since the lattice constant in the vertical direction is $\sim 2.0\%$ less than the lattice constant in the horizontal direction.

Finally, we observe columnar crystal growth and no dense amorphous sediment for $\phi^* < \phi_f^*$, while the computer simulations of microsphere sedimentation by Davis and Russel[15] produce mixed-crystal and amorphous sediments for samples of similar reduced variables (Peclet number and volume fraction) in agreement with experiments on silica suspensions. This difference indicates the possibility of experimental polydispersity in particle size in the silica systems or a lack of hardness in our spheres. In conclusion, we have measured $K(\phi^*)$ for a system of hard spheres using the equilibrium phase transition as a unique marker for the volume fraction in concentrated systems. We find $K(\phi_f^*) = 0.026$ and $K(\phi_m^*) = 0.016$.

We wish to thank J. F. Brady and P. N. Pusey for their insightful discussions. This work is supported by U.S. Department of Energy Grant No. DE-FG05-88ER45349.

[1]B. J. Alder, W. G. Hoover, and D. A. Young, J. Chem Phys. **49**, 3688 (1968).

[2]B. B. Laird, J. D. McCoy, and A. D. J. Haymet, J. Chem. Phys. **87**, 5549 (1987).

[3]E. Thiele, J. Chem. Phys. **39**, 474 (1963).

[4]Norman F. Carnahan and Kenneth E. Starling, J. Chem. Phys. **51**, 635 (1969).

[5]R. Zwanzig, J. Chem. Phys. **22**, 1420 (1954).

[6]J. A. Barker and D. Henderson, Annu. Rev. Phys. Chem. **23**, 439 (1972).

[7]J. D. Weeks, D. Chandler, and H. C. Andersen, J. Chem. Phys. **54**, 5237 (1971).

[8]P. N. Pusey and W. van Megen, in *Complex and Supermolecular Fluids,* edited by S. A. Safran (Wiley-Interscience, New York, 1987).

[9]C. G. de Kruif, P. W. Rouw, J. W. Jansen, and A. Vrij, J. Phys. (Paris), Colloq. **46**, C3-295 (1985).

[10]J. W. Jansen, C. G. de Kruif, and A. Vrij, J. Colloid Interface Sci. **114**, 501 (1986).

[11]M. M. Kops-Werkhoven, C. Pathmamanoharan, A. Vrij, and H. M. Fijnaut, J. Chem. Phys. **77**, 5913 (1982).

[12]M. M. Kops-Werkhoven and H. M. Fijnaut, J. Chem. Phys. **74**, 1618 (1981).

[13]M. M. Kops-Werkhoven and H. M. Fijnaut, J. Chem. Phys. **77**, 2242 (1982).

[14]G. K. Batchelor, J. Fluid Mech. **74**, 1 (1976).

[15]K. E. Davis and W. B. Russel, Adv. Ceram. **21**, 573 (1987).

[16]John F. Brady, Ronald J. Phillips, Julia C. Lester, and Georges Bossis, J. Fluid Mech. **195**, 257 (1988).

[17]B. Cichocki and B. U. Felderhof, Physica (Amsterdam) **154A**, 213 (1989).

[18]C. W. J. Beenakker and P. Mazur, Physica (Amsterdam) **126A**, 349 (1984).

[19]A. D. Maude and R. L. Whitmore, Br. J. Appl. Phys. **9**, 477 (1958).

[20]C. C. Reed and John L. Anderson, AIChE J. **26**, 816 (1980).

[21]R. Buscall, J. W. Goodwin, R. H. Ottewill, and Th. F. Tadros, J. Colloid Interface Sci. **85**, 78 (1982).

[22]K. E. Davis, W. B. Russel, and W. J. Glantsching, Science **245**, 507 (1989).

[23]P. N. Pusey and W. van Megen, Nature (London) **320**, 340 (1986); Phys. Rev. Lett. **59**, 2083 (1987).

[24]Bruce J. Ackerson and P. N. Pusey, Phys. Rev. Lett. **61**, 1033 (1988).

[25]J.-C. Bacri, C. Frénois, M. Hoyos, R. Perzynski, N. Rakotomalala, and D. Salin, Europhys. Lett. **2**, 123 (1986).

[26]A. A. Zick and G. M. Homsy, J. Fluid Mech. **115**, 13 (1982).

[27]H. Hasimoto, J. Fluid Mech. **5**, 317 (1959).

[28]P. G. Saffman, Stud. Appl. Math. **102**, 115 (1973).